

# Preparation of Carbon Dots with Ultrahigh Fluorescence Quantum Yield Based on PET Waste

Yuhang Wu,<sup>||</sup> Guocong Ma,<sup>||</sup> Anying Zhang, Weiwen Gu, Jianfei Wei,<sup>\*</sup> and Rui Wang<sup>\*</sup>Cite This: *ACS Omega* 2022, 7, 38037–38044

Read Online

ACCESS |



Metrics &amp; More

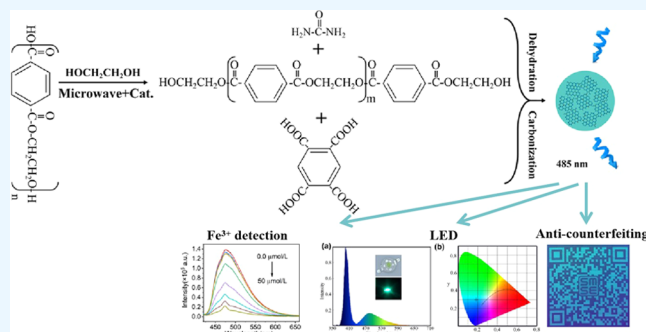


Article Recommendations



Supporting Information

**ABSTRACT:** Environmentally friendly polyethylene terephthalate-based carbon dots (PET-CDs) with ultrahigh fluorescence quantum yield were prepared with waste PET textiles as raw materials. First, oligomers were prepared from the reaction of waste PET textile and ethylene glycol by the microwave method. Then, the mixture without isolation and purification as well as pyromellitic acid and urea were adopted as precursors for the preparation of PET-CDs by the hydrothermal method. It was found that the as-prepared PET-CDs had a spherical structure with an average particle size of 2.8 nm. The carbon core of PET-CDs was a graphene-like structure doped with nitrogen atoms in the form of pyrrole nitrogen and the surface contained  $-\text{NH}_2$ , which is convenient for modification and functionalization with various materials in the form of chemical bonds. The as-prepared PET-CDs exhibit excitation-independent emission properties in the range from 340 to 440 nm, and the best excitation and emission wavelengths of PET-CDs are 406 and 485 nm, respectively, while the fluorescence quantum yield is 97.3%. In terms of the application, the as-prepared PET-CDs could be adopted as a fluorescence probe for the detection of  $\text{Fe}^{3+}$ , and the limit of detection is as low as  $0.2 \mu\text{mol/L}$ . The mechanism of PET-CDs by  $\text{Fe}^{3+}$  was found to be the static quenching mechanism. In addition, PET-CDs can be used in LEDs and fluorescent anticounterfeiting.



## 1. INTRODUCTION

Polyethylene terephthalate (PET) is a semicrystalline thermoplastic polymer material, which is one of the most used plastics in the worldwide by virtue of lightweight, durability, excellent wear, and chemical resistance coupled with the low market price. The production and consumption of PET products in the world have increased remarkably in recent years. The global consumption value of PET is expected to reach \$68 billion in 2023.<sup>1</sup> Disposable PET packaging, such as water bottles, soft drink bottles, food containers, and so on, is found in wide applications due to its excellent barrier against moisture, oxygen, and carbon dioxide. The application of PET in disposable beverage bottle accounts for about 70% of the total market segments, and more than 500 billion PET bottles are used worldwide each year. Meanwhile, the PET fiber known as terylene is used widely in the textile industry by the virtue of its high strength, high modulus, good resilience, good wear resistance, low water absorption, strong chemical stability, and other excellent properties. In 2021, the output of terylene in China exceeded 50 million tons, which is the first big variety of the synthetic fiber at present and accounts for about 80% of the annual output of the chemical fiber in China. The widespread application and extensive consumption of PET in the packaging, textile fields, and other fields generate plenty of PET waste and come at a great cost to the environment due to the slow natural decay of PET materials

and their poor waste disposal management. A study published by Nature Communications showed that about 92% of microplastic pollution in the Arctic's near-surface waters comes from synthetic fibers.<sup>2</sup> Of these, about 73% is polyester, similar to the fibers used in textiles. Therefore, the recycling of PET waste, especially PET textile waste, is of great significance in solving the environmental pollution and shortage of petrochemical resources caused by the poor recycling of PET waste.

Common PET recovery methods can be simply divided into mechanical recycling and chemical recycling. The typical characteristics of mechanical recycling are simple and flexible. In addition, the investment in the mechanical recycling of PET is low because the established equipment can be utilized in the process of mechanical recycling. However, PET from mechanical recycling plants exhibits relatively low molecular weight and intrinsic viscosity values due to the degradation during the reprocessing, which prevents the value-added

Received: August 19, 2022

Accepted: September 30, 2022

Published: October 13, 2022



application of recycled PET. Chemical recycling is another accepted pathway for reusing PET waste, which generates monomers of PET and other value-added micromolecules for various industrial and commercial applications. However, PET prepared from monomers of chemical recycling is more expensive than virgin PET. Thus, it is of great significance to develop a simple, sustainable, economical, and ecofriendly way to implement waste PET recycling. A promising PET recycling process is the enzymatic or microbial biodegradation of PET waste to its monomers. Several PET hydrolase enzymes have been reported.<sup>3–9</sup> André, Duquesne, and Marty reported an improved PET hydrolase, which can degrade 200 g of PET plastic in 10 h with a concentration of 3 mg hydrolase per gram of PET.<sup>3</sup> Another promising method for the recycling of PET waste is to implement waste PET upcycling to value-added products. Duan and co-worker reported electrocatalytic upcycling of PET plastic to valuable potassium diformate, terephthalic acid, and H<sub>2</sub> fuel.<sup>10</sup> Waldow, Freire, and Castro provide a promising strategy to convert PET waste into N-doped porous carbon as a CO<sub>2</sub> adsorbent and a solar steam generator, which exhibits a high CO<sub>2</sub> uptake of 6.47 mmol g<sup>-1</sup> with a CO<sub>2</sub>/N<sub>2</sub> selectivity of 89 and a high evaporation rate of 1.62 kg m<sup>-2</sup> h<sup>-1</sup> with a conversion efficiency of 91.6%.<sup>11</sup>

Carbon dots (CDs) are a class of zero-dimensional carbon nanomaterials with a size of less than 20 nm, which is composed of a sp<sup>2</sup>/sp<sup>3</sup> carbon core and oxygen/nitrogen functional groups on the surface. Due to low cost and simple preparation, good biocompatibility, low cell toxicity, excellent photoluminescence, and adjustable emission wavelengths, it has great application potential in the fields of sensors, catalysis, biomedicine, biological imaging, light-emitting diodes (LEDs), fluorescent inks, and other fields.<sup>12–15</sup> More importantly, CDs have a wide range of raw materials. Theoretically, all substances containing carbon atoms can become the raw materials of CDs. In terms of the chemical structure and composition, PET contains a large number of benzene rings, and the carbon content of PET is high. As a result, PET is an ideal precursor for CDs. Heteroatom doping is a common strategy for the preparation of CDs because the doping of heteroatoms can effectively change the composition and surface structure of CDs, leading to the improvement of the optical properties of CDs. Therefore, the preparation of heteroatom-doped CDs with PET as a precursor can not only solve the recycling problem of PET waste but also greatly improve the added value of PET waste.

In this study, PET-based carbon dots (PET-CDs) with ultrahigh fluorescence quantum yield were prepared with waste PET textiles as raw materials. First, oligomers were prepared from the reaction of waste PET textile and ethylene glycol by the microwave method. Then, the mixture without isolation and purification as well as pyromellitic acid and urea were adopted as precursors for the preparation of PET-CDs by the hydrothermal method. The morphology and structure of PET-CDs were studied by transmission electron microscopy (TEM), Fourier transform infrared spectrometry (FTIR), X-ray photoelectron spectroscopy (XPS), and nuclear magnetic resonance (NMR). After that, the fluorescence performance of PET-CDs was investigated, and its applications in Fe<sup>3+</sup> detection, LEDs, and fluorescence anticounterfeiting were explored.

## 2. MATERIALS AND METHODS

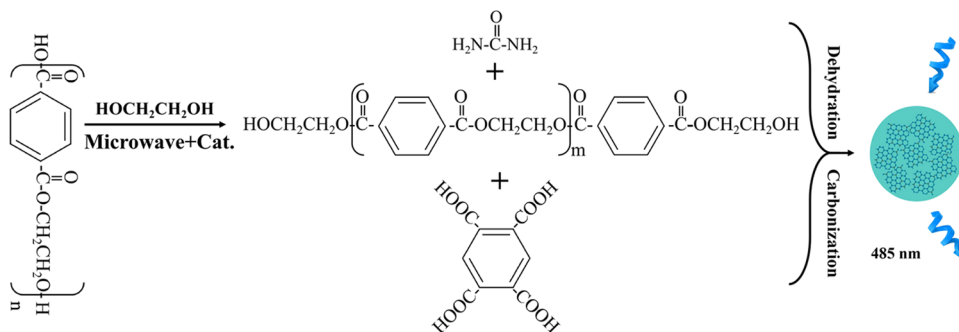
**2.1. Chemicals.** Waste PET fibers came from Shanghai Different Advanced Material Company Limited. Ethylene glycol was of industrial grade, provided by Sinopec Tianjin Branch. Analytically pure ammonia (25–28%), hydrochloric acid (36–38%), NaOH, and BaCl<sub>2</sub> were purchased from Beijing Chemical Plant. Hg(NO<sub>3</sub>)<sub>2</sub>·H<sub>2</sub>O, Pb(NO<sub>3</sub>)<sub>2</sub>, CrCl<sub>2</sub>, CaCl<sub>2</sub>, KI, NaCl, LiCl, (CH<sub>3</sub>COO)<sub>2</sub>Zn·2H<sub>2</sub>O, and glycerol, analytically pure, were obtained from Beijing Tongguang Fine Chemical Company. Urea, terephthalic acid, FeCl<sub>3</sub>, ZnCl<sub>2</sub>, and polyvinyl alcohol 1788 low viscosity type (alcohol lysis: 87.0–89.0 (mol/mol), CPS: 4.6–5.4), analyzed purely, were purchased from Shanghai Macklin Biochemical Technology Co., Ltd. CuCl<sub>2</sub> and Cd(NO<sub>3</sub>)<sub>2</sub>, analytically pure, were obtained from Tianjin Fuchen Chemical Reagent Factory. Analytically pure AgNO<sub>3</sub> was purchased from Shanghai Aladdin Biochemical Technology Co., Ltd. Fetal bovine serum was purchased from Biological Industries. Analytically pure dimethyl sulfoxide (DMSO) was obtained from Tianjin Fuyu Fine Chemical Co., Ltd. A phosphate-buffered salt solution (PBS) was obtained from Wuhan Punuosai Life Technology Co., Ltd. MTT was purchased from Beijing Solebao Technology Co., Ltd. Hela cells were supplied by Shanghai Cybertron Biotechnology Co., Ltd. Deionized water was laboratory-made.

**2.2. Apparatus.** An analytical balance (LS 120A scs), Swiss Precisa; a microwave reactor (MCR-3), Beijing Berlin Yuanhang Technology Co., Ltd; an electric constant temperature blast drying box (DHG-9075AL), Beijing Luxi Technology Co., Ltd; a vacuum freeze dryer (FD-1A-50), Beijing Boyikang Experimental Instrument Co., Ltd; a fluorescence spectrometer (FSS), Edinburgh Instruments, U.K.; a transmission electron microscope (FEI Tecnai G2 F30), FEI Company; a Fourier transform infrared spectrometer (Nicolet Nexus 670), Nicolet Corporation of America; an X-ray photoelectron spectroscopy (250Xi), Thermo Scientific Corporation; a printer (Desk Jet2132HP), HP China; a CO<sub>2</sub> incubator (WIGGENS WCI-180), Beijing Sangyi Institute of Experimental Instruments; a centrifuge (TDS), Shanghai Lu Xiangyi Centrifuge Instrument Co., Ltd; a microplate reader (SPARK 10M), TECAN, Switzerland; and a multifunctional spectrometer (model: OHSP350M with 0.3 m integrating sphere), Hangzhou Rainbow Spectrum Light Color Technology Co., Ltd were used in the experiments.

**2.3. Experimental Methods.** **2.3.1. Synthesis of PET-CDs.** The waste PET fiber (48 g), ethylene glycol (14 g), and zinc acetate dehydrate (0.4 g) were added to a round-bottom flask, which was placed in a microwave reactor (540 W) for 20 min. The above solution was poured into a beaker while it was hot, cooled to room temperature, and crushed into powder with a pulverizer, which was the mixture of BHET and a small amount of oligomers.

PET-CDs were prepared by the hydrothermal method with the as-prepared mixture, urea, and homophthalic acid as precursors. The specific preparation procedure was that the as-prepared mixture (2 g), urea (1g), and homophthalic acid (0.7) were added to a 100 mL polyphenylene-lined stainless-steel autoclave. Subsequently, the autoclave was placed in a 260 °C blast drying chamber for 24 h. After the autoclave cooled to room temperature, the large particles in the as-prepared suspension were filtered with a 0.22 μm injection syringe filter to obtain an aqueous solution of PET-CDs. The

Scheme 1. Mechanism for the Preparation of PET-CDs with PET as a Precursor



aqueous solution of PET-CDs was dialyzed using dialysis using a 1 kDa dialysis bag for 24 h, during which the deionized water was replaced every 4 h. After the dialysis was completed, the PET-CD powder was freeze-dried and set aside.

**2.3.2. Cytotoxicity Experiment.** HeLa cells were seeded into 96-well plates and cultured in a 5% CO<sub>2</sub>, 37 °C incubator until the cells adhered. Different concentrations of a PET-CD cell culture medium (0–400 μg mL<sup>-1</sup>) were injected into the 96-well plate and incubated for 24 h, and the medium containing the samples was removed. Each well was washed three times with PBS, and 100 μL of the medium containing 0.5 mg mL<sup>-1</sup> MTT was added to each well, 5% CO<sub>2</sub>, and incubated for 4 h in a constant temperature incubator at 37 °C. The supernatant was discarded, and 100 μL of DMSO was added to each well. The absorbance at 570 nm was detected after shaking gently for 10 min.

**2.3.3. Metal Ion-Sensing Analysis.** First, the as-prepared PET-CD solution was diluted 200-fold. Overall, 10 μL of the diluted PET-CD solution and 1.99 mL of a metal ion solution were added to a four-way colorimeter with a pipette. The fluorescence emission spectrum was determined after 1 min of mixing in FSS. The specific parameters are as follows: the excitation wavelength is 408 nm, the emission wavelength is measured in the range of 420–660 nm, and the slit width is 3 and 6 nm, respectively.

A linear relationship is established between Δ*F* and the concentration of Fe<sup>3+</sup> in an aqueous solution. In an aqueous solution without Fe<sup>3+</sup>, the fluorescence intensity for the emission peak (485 nm) of PET-CDs was defined as *F*<sub>0</sub>. The fluorescence intensity for the emission peak (485 nm) of PET-CDs in an Fe<sup>3+</sup> aqueous solution with different concentrations was defined as *F*<sub>*t*</sub>, and the difference between *F*<sub>0</sub> and *F*<sub>*t*</sub> was denoted as Δ*F*.

**2.3.4. Preparation of LEDs.** PET-CD lyophilized powder of PET-CDs was added to a 15% poly(vinyl alcohol) (PVA) aqueous solution, and the mass ratio of PET-gCDs and PVA was 16:84. Then, the mixture in a glass bottle with a lid was placed in 80 °C hot water for 60 min ultrasonication with a glass rod stirring from time to time. Finally, a uniform mixed solution was obtained and cooled to room temperature for standby.

Overall, 20 μL of the resulting solution was dropwise added onto a 395 nm ultraviolet (UV) LED chip with a pipette, which was then placed in a fume hood. After the moisture was completely volatilized, the LED device was finally prepared.

**2.3.5. Preparation of Fluorescent Ink.** The PET-CDs were dissolved in deionized water to prepare a 1 mg mL<sup>-1</sup> dispersion, which was injected into the washed cartridge for an inkjet printer (Desk Jet2132HP) with a syringe, and then

the selected pattern was printed on paper without a fluorescent background.

### 3. RESULTS AND DISCUSSION

**3.1. Preparation of PET-CDs.** Heteroatom doping is an effective method to prepare CDs with excellent optical and chemical properties by tuning their carbon skeleton matrices and chemical structures. Among these, nitrogen-doped CDs have attracted remarkable attention for their potential analytical and biological applications as they display excellent optical, electrical, and chemical properties. The majority of synthesis methods of nitrogen-doped CDs are hydrothermal methods, in which the elevated temperature and pressure conditions favor doping of the carbon core structure with nitrogen and the as-prepared nitrogen-doped CDs have a uniform size and high quantum yield.<sup>14</sup> In this paper, nitrogen-doped CDs with PET waste as a precursor (PET-CDs) were prepared, in which the alcoholysis reaction of PET waste with ethylene glycol was carried out by the microwave method for the production of oligomers,<sup>1</sup> and the product mixed with pyromellitic acid, urea, and water was put into the autoclave. The mechanism for the preparation of PET-CDs generally includes dehydration, cross-linking, and carbonization of precursors, resulting in the formation of aromatic polymers (Scheme 1). When the concentration of these aromatic polymers crosses a supersaturation point, they undergo a burst of nucleation and the formation of PET-CDs. Through a series of comparative experiments (Figure S1), it is found that BHET, pyromellitic acid, and urea are indispensable for the preparation of PET-CDs, that is to say, that the synergistic effect of BHET, pyromellitic acid, and urea resulted in the successful preparation of PET-CDs.

**3.2. Morphological Characteristics of PET-CDs.** The as-prepared PET-CDs were characterized by transmission electron microscopy (TEM), and the results were shown in Figure 1. According to Figure 1a, it can be seen that PET-CDs is spherical, and well dispersed, and there is no agglomeration. The diameter of the as-prepared PET-CDs is in the range from 1.6 to 4.6 nm with an average size of 2.8 nm (Figure 1b). What is more, it can be seen from the inset of Figure 1a that the well-resolved lattice spacing of PET-CDs is 0.21 nm, which is consistent with the *d*-spacing of the graphene (100) planes.<sup>16</sup>

**3.3. Structural Properties of PET-CDs.** The possible chemical bonds and surface functional groups of PET-CDs were thoroughly investigated by infrared spectroscopy (FTIR), X-ray photoelectron spectroscopy (XPS) and nuclear magnetic resonance hydrogen spectroscopy (<sup>1</sup>H NMR). The FTIR spectrum of PET-CDs is shown in Figure 2a. PET-CDs exhibited broad absorption bands centered at 3019 cm<sup>-1</sup>

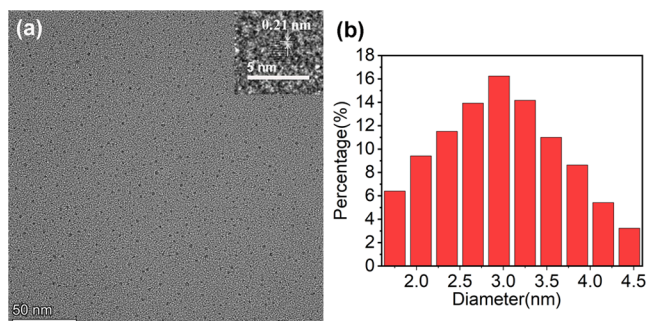


**Figure 1.** (a) TEM image of PET-CDs (the inset shows the high-resolution TEM images of PET-CDs); (b) size distribution graph of PET-CDs corresponding to (a).

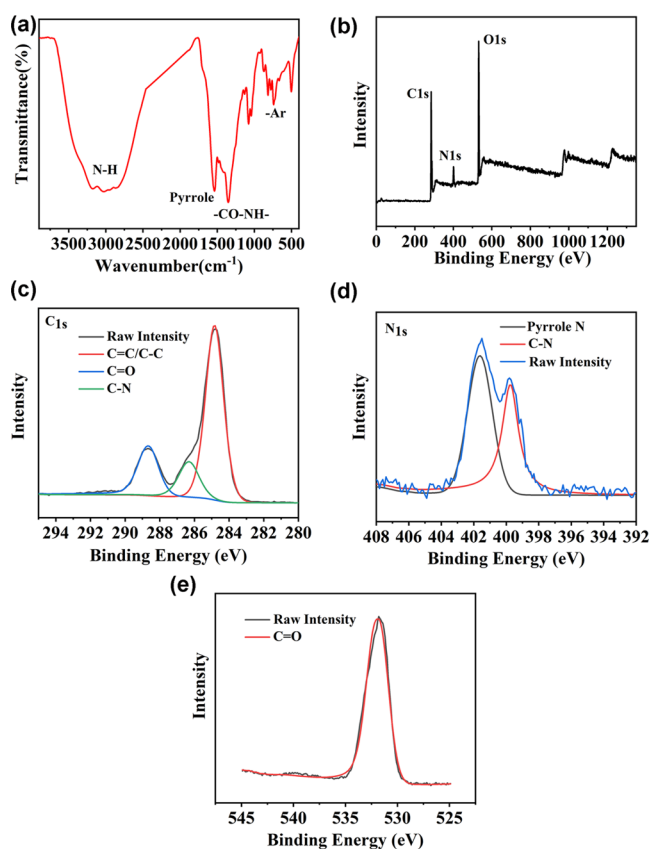


**Figure 2.** (a) FTIR of PET-CDs, (b) XPS full spectrum of PET-CDs, (c) C 1s spectra of PET-CDs, (d) N 1s spectra of PET-CDs, and (e) O 1s spectra of PET-CDs.

attributed to the stretching vibrations of the N–H and O–H group. The observed band at  $727\text{ cm}^{-1}$  is correspond to the occurrence of the –Ar group. The presence of stretching CO–NH group was confirmed by the band appeared at  $1342\text{ cm}^{-1}$ , while the characteristic peaks at  $1528\text{ cm}^{-1}$  indicated the existence of the pyrrole group. It was demonstrated according to the FTIR that PET-CDs contains abundant functional group such as Pyrrole, N–H, CO–NH and –Ar depending upon the raw materials. XPS is also used to analyze the structure of PET-CDs. The full spectrum of XPS is shown in (Figure 2b), and it can be found that there are three typical binding peaks at 284.8, 401.2, and 532.0 eV, representing the binding energy peaks of C 1s, N 1s, and O 1s. That is to say that the synthesized PET-CDs mainly contain C, N, and O

elements. The atomic percentages of C, N, and O were respectively 62.65, 8.13, and 29.21%, indicating the successful doping of nitrogen for the PET-CDs. It can be found that the high-resolution C 1s spectrum can be fitted with three peaks at 284.8, 286.3, and 288.8 eV, representing C=C/C–C bonds, C=O bonds, and C–N bonds.<sup>17</sup> In addition, the presence of C=O bonds can be seen in the O 1s spectrum (Figure 2e).<sup>18</sup> The high-resolution N 1s spectrum was deconvoluted into two peaks with the binding energies at 399.8 and 401.6 eV, corresponding to C–N and pyrrole N.<sup>19</sup> The above results are in good accordance with the result of FTIR analysis. To sum up, the as-prepared PET-CDs was not only successfully doped with nitrogen in the form of pyrrole N structures but also was covered with –NH<sub>2</sub> and abundant oxygen-containing functional group, which makes it easy to combine with various materials for modification and functionalization in the form of chemical bonds.

**3.4. Optical Properties of PET-CDs.** The optical properties of PET-CDs were investigated by fluorescence spectrometry (FSS), and the results are demonstrated in Figure 3. It can be found from Figure 3a that the as-prepared PET-

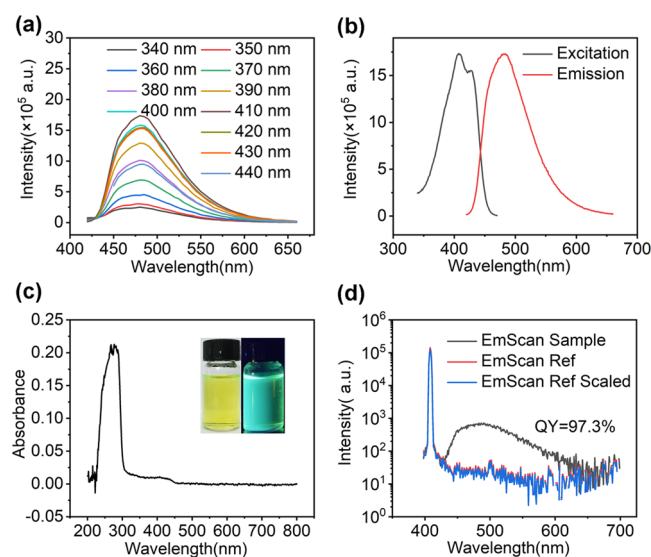


**Figure 3.** (a) Fluorescence emission spectra of PET-CDs at different excitation wavelengths in the range of 340–440 nm, (b) excitation and emission spectra of PET-CDs, and (c) UV–vis absorption spectrum of PET-CDs; the inset shows the photographs of the as-prepared PET-CD solutions under natural light (left) and 365 nm ultraviolet light (right) and (d) fluorescence quantum yield of PET-CDs.

CDs exhibit excitation-independent emission properties. In other words, the position of the emission peak does not change with the change in the excitation wavelength in the range of 340–440 nm, and the optimal emission wavelength is always 485 nm, which is similar to the result of Figure 3b. The optimal excitation wavelength of the PET-CDs is 406 nm according to the excitation spectrum (485 nm emission) in Figure 3b, and it can be found that the Stokes shift is 79 nm. The absorption peaks at 282 nm in the UV–visible (UV–vis) absorption spectrum of PET-CDs (Figure 3c) indicate the formation of a graphite carbon structure for PET-CDs,<sup>20</sup> while absorption peaks at 406 nm are consistent with the optimal emission wavelengths. In addition, the absolute fluorescence quantum yield of PET-CDs was measured by the integrating sphere

attachment, and the results were as high as 97.3% (Figure 3d), close to the theoretical maximum (100%).

**3.5. Cytotoxicity of PET-CDs.** The high aqueous solubility and outstanding fluorescence of PET-CDs promote us to investigate the cytotoxicity of PET-CDs. As a result, the MTT-mediated cell viability assay was conducted with HeLa cells. It can be found that the relative cell viability decreased with the increase in the concentration of PET-CDs and 75% of the cells remained biologically active even at a PET-CD concentration of  $400 \mu\text{g mL}^{-1}$  (Figure 4a) after incubation of PET-CDs with

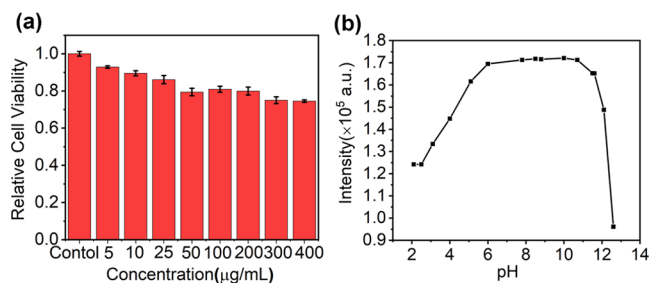


**Figure 4.** (a) MTT assay to analyze the biotoxicity of PET-CDs in cervical cancer (HeLa) cells. (b) Effect of solution pH on PET-CDs.

HeLa cells for 24 h. The MTT assay demonstrated that PET-CDs prepared from PET waste are a strong candidate for biological and biosensing applications as nontoxic materials.<sup>21</sup> In addition, it can be found from Figure 4b that the fluorescence intensity of PET-CDs remains stable when excited at 406 nm in the pH range of 6–11, so it has the potential for biological and biosensing applications.

All of the above-mentioned features suggest that the as-prepared PET-CDs have wide applications in various fields and under different conditions.

**3.6. Application of PET-CDs in  $\text{Fe}^{3+}$  Detection.**  $\text{Fe}^{3+}$  is an essential trace metal for organisms, which has a high affinity for oxygen, and plays a leading role in electron transport and oxygen metabolism.<sup>22,23</sup> Both deficiency and excess iron can cause various biological disorders that interfere with intracellular homeostasis. Therefore, the detection of  $\text{Fe}^{3+}$  is essential for health. PET-CDs prepared in this study are capable of specifically identifying  $\text{Fe}^{3+}$  (Figure 5a), and their fluorescence intensity gradually decreases as  $\text{Fe}^{3+}$  concentration increases (Figure 5b). As can be seen from Figure 5c,d, fluorescence quenching of PET-CDs ( $\Delta F$ ) is linearly dependent on the  $\text{Fe}^{3+}$  concentrations in the range of 0–15  $\mu\text{mol L}^{-1}$  ( $R^2 = 0.9929$ ), and the detection can reach  $0.05 \mu\text{mol L}^{-1}$ , which is similar to other literature reports.<sup>24,25</sup>

To further confirm the feasibility of the application of PET-CDs in the detection of  $\text{Fe}^{3+}$ , the proposed fluorescent turn-off sensor was adopted to detect the concentration of  $\text{Fe}^{3+}$  with the intentional addition of 4 or 10  $\mu\text{M}$  in tap water. It was found that the recoveries of  $\text{Fe}^{3+}$  in tap water were  $97.6 \pm 1.2$  and  $99.8 \pm 1.0\%$ , respectively. Therefore, the feasibility of the application of PET-CDs in the detection of  $\text{Fe}^{3+}$  in real samples was confirmed.

The fluorescence quenching mechanism can be divided into the following four types:<sup>26–29</sup> (1) the internal filter effect quenching mechanism: the added substance can absorb the excitation light of the fluorescent probes or absorb the emitted light of the fluorescent probes so that the fluorescent probes cannot be excited or the emitted light cannot be released; (2) dynamic quenching mechanism: the fluorescent probes in the

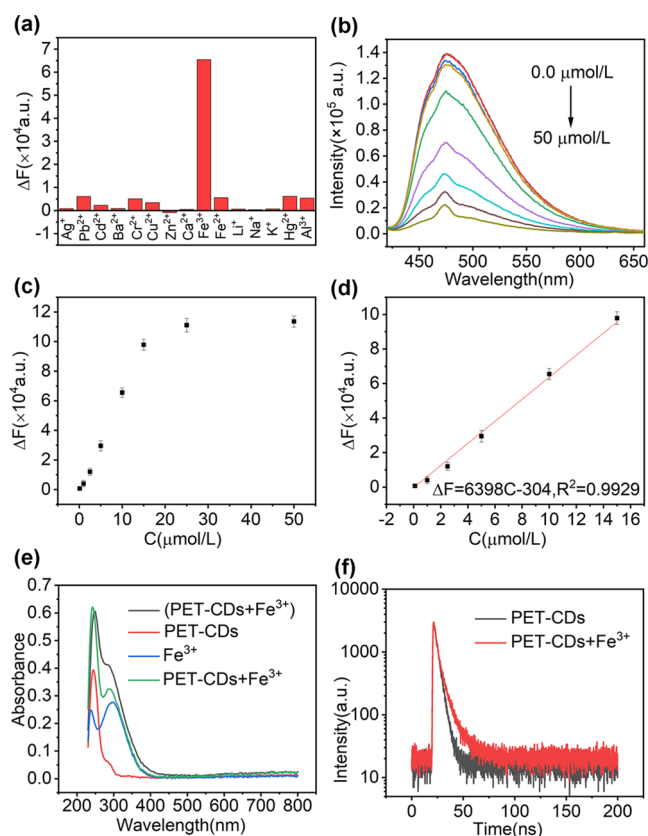


**Figure 5.** (a) Fluorescence quenching of PET-CDs ( $\Delta F$ ) before and after the addition of  $10 \mu\text{mol L}^{-1}$  of different metal ions ( $\Delta F = F_0 - F_t$ ,  $F_0$  is the fluorescence intensity at 485 nm before the addition of metal ions,  $F_t$  is the fluorescence intensity at 485 nm after the addition of ions); (b) emission spectrum of PET-CDs excited by the light of 406 nm in the  $\text{Fe}^{3+}$  solution with different concentrations (0, 0.1, 2.5, 5, 10, 15, 25, 50, 75  $\mu\text{mol L}^{-1}$ ); (c) correspondence between  $\Delta F$  and  $\text{Fe}^{3+}$  concentrations; (d) linear relationship between  $\Delta F$  and  $\text{Fe}^{3+}$  concentrations; (e) UV–vis spectra of PET-CDs and  $\text{Fe}^{3+}$  mixtures, PET-CDs, and  $\text{Fe}^{3+}$ ; and (f) fluorescence lifetime of PET-CDs (excitation wavelength-406 nm, emission wavelength-485 nm) before and after quenching by  $\text{Fe}^{3+}$  ( $50 \mu\text{mol L}^{-1}$ ).

excited state have a certain collision effect with the added material, and the excited fluorescent probes lose the excitation energy and return to the ground state, causing the quenching of the fluorescence; (3) static quenching mechanism: the quenching of fluorescence was caused by chemical reactions between the fluorescent probes and the added substance to form a nonfluorescent substance; and (4) the combination of dynamic and static quenching mechanisms: the fluorescence of the probe can not only be dynamically quenched but also static quenched by the added substance.

From the UV–vis absorption spectra in Figure 5e, it can be seen that  $\text{Fe}^{3+}$  as the detection substance has almost no absorption in the range of 400–800 nm, so it can be confirmed that the mechanism of  $\text{Fe}^{3+}$  quenching CDs is not the inner filter effect quenching mechanism. In addition, the quenching mechanism could be distinguished by the UV–vis absorption spectra of fluorescent probes before and after quenching. The UV–vis absorption spectra change for the fluorescent probes quenched due to static quenching mechanism or combined quenching mechanism due to the formation of a non-fluorescent substance, while the UV–vis absorption spectra remain the same for the fluorescent probes quenched due to

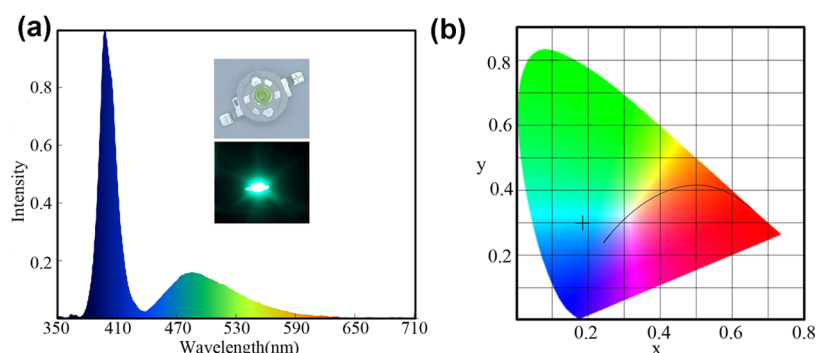


**Figure 6.** Spectrogram (a) and color coordinate diagram (CIE 1931) of the device assembled with PET-gCDs and 395 nm LED chips (the inset in (a) shows the actual image of the device (top) and the luminescence photograph at 3.0 V).

the dynamic quenching mechanism. It can be speculated from Figure 5e that the quenching mechanism of PET-CDs by  $\text{Fe}^{3+}$  is the static quenching mechanism or the combined quenching mechanism. In addition, the static quenching mechanism, the dynamic quenching mechanism, and the combination can be judged by testing whether the fluorescence lifetime changed for the fluorescent probes before and after the quenching. If the fluorescence lifetime of fluorescent probes changes, it can be speculated that the quenching mechanism is the dynamic quenching mechanism or the combined quenching mechanism. If the fluorescence lifetime of fluorescent probes remains the same, it indicates that the quenching mechanism is the static quenching mechanism. As shown in Figure 5f, the fluorescence life for PET-CDs before and after being quenched by  $\text{Fe}^{3+}$  ( $50 \mu\text{mol L}^{-1}$ ) did not change significantly. The average fluorescence life before and after the quenching of PET-CDs by  $\text{Fe}^{3+}$  is 5.84 and 5.93 ns, respectively, so it can be determined that the quenching mechanism is the static quenching mechanism. In summary, it can be demonstrated from the results of UV-vis and the fluorescent lifetime that the quenching mechanism of PET-CDs by  $\text{Fe}^{3+}$  is the static quenching mechanism.

**3.7. Application of PET-CDs in LEDs.** Light-emitting diodes (LEDs) are a kind of solid-state lighting equipment, which can efficiently convert electrical energy into light energy. LEDs are considered to be a green light source in the 21st century by the virtue of their long life, high efficiency and energy saving, simple structure, small size, lightweight, fast response, low working voltage, and good safety. At present, the commonly used phosphors are mainly rare-earth fluorescent materials and semiconductor quantum dots. However, they are toxic to human beings and the environment and come from limited sources of raw materials.<sup>30–32</sup> Therefore, it is important to develop fluorescent materials with a wide range of raw material sources and good biocompatibility. CDs are fluorescent materials that could replace traditional phosphors because of their wide range of raw material sources, good biocompatibility, and excellent fluorescence properties. The as-prepared PET-CDs have the characteristics of nonexcitation wavelength dependence; the optimal excitation wavelength is 406 nm and the optimal emission wavelength is 485 nm so that it can be used as a phosphor for 395 nm UV LED chips. Since the PET-CDs are fluorescently quenched in solid states, PVA, which can be dissolved in water, is chosen as the dispersion medium. Figure 6a shows a spectrogram of an LED device assembled from PET-CDs dispersed in a PVA matrix and a 395 nm LED chip, illustrated as a picture of the device (top) and a

luminescence photograph at a voltage of 3.0 V. As can be seen from Figure 6a, the emission spectrum of the LED device contains two emission peaks: one of the peaks is at 395 nm, which is the emission peak of the ultraviolet chip, and the other wide peak centered at 485 nm is the emission peak from the PET-CDs, which is blue-green light. Figure 6b shows the color coordinate diagram (CIE 1931) of the prepared LED chip; the color coordinate is (0.18, 0.30), and the associated color temperature is 36,925 K.

**3.8. Application of PET-CDs in Fluorescence Anti-counterfeiting.** Injecting an aqueous solution of PET-CDs into the ink cartridge of the inkjet printer, various fluorescent patterns can be quickly printed on paper without a fluorescent background. Printed patterns cannot be observed in natural light, while clear fluorescent patterns (Figure 7) can be



**Figure 7.** Picture of a pattern printed in fluorescent ink with a PET-CD solution under a 365 nm ultraviolet light.

observed under UV light at 365 nm, and the printed patterns are full and clearly detailed. The printed QR code can be quickly scanned and recognized through WeChat, which proves that the pattern is clear and recognizable. This proves that PET-CDs can be applied to fluorescence security.

## 4. CONCLUSIONS

In this paper, PET-based carbon dots (PET-CDs) with ultrahigh fluorescence quantum yield were prepared with waste PET textiles as raw materials. The results show that PET-CDs have a spherical structure with an average particle

size of 2.8 nm. The carbon core of PET-CDs was a graphene-like structure doped with nitrogen atoms in the form of pyrrole nitrogen, and the surface contained  $-\text{NH}_2$ , which is convenient for modification and functionalization with various materials in the form of chemical bonds. The best excitation and emission wavelengths of PET-CDs are 406 and 485 nm, respectively, and the fluorescence quantum yield is 97.3%. The fluorescence intensity of PET-CDs remains stable in the range of a certain pH (6–11), and the cytotoxicity is low. All of the above-mentioned features suggest that the as-prepared PET-CDs have wide applications in various fields and under different conditions. The fluorescence intensity of PET-CDs can be selectively quenched by  $\text{Fe}^{3+}$ , and the detection limit is as low as  $0.2 \mu\text{mol L}^{-1}$ . The mechanism of PET-CDs by  $\text{Fe}^{3+}$  was found to be the combined quenching mechanism of static and dynamic. In addition, PET-CDs can be used in LEDs and fluorescent anticounterfeiting. Exploring the preparation of CDs with PET waste as a precursor is conducive to solving the shortage of petrochemical resources and environmental pollution problems but also provides a reference for high-value-added recycling of PET.

## ■ ASSOCIATED CONTENT

### SI Supporting Information

The Supporting Information is available free of charge at <https://pubs.acs.org/doi/10.1021/acsomega.2c05324>.

Fluorescence intensity of PVA films with different PET-CDs concentrations and spectrogram of the 395 nm LED chips and the device assembled with PET-gCDs and 395 nm LED chips (PDF)

## ■ AUTHOR INFORMATION

### Corresponding Authors

**Jianfei Wei** – School of Materials Design and Engineering, Beijing Institute of Fashion Technology, Beijing 100029, China; Beijing Key Laboratory of Clothing Materials R&D and Assessment, Beijing Engineering Research Center of Textile Nano Fiber, Beijing Institute of Fashion Technology, Beijing 100029, China; [orcid.org/0000-0003-4834-8623](https://orcid.org/0000-0003-4834-8623); Email: [weijianfei@bift.edu.cn](mailto:weijianfei@bift.edu.cn)

**Rui Wang** – School of Materials Design and Engineering, Beijing Institute of Fashion Technology, Beijing 100029, China; Beijing Key Laboratory of Clothing Materials R&D and Assessment, Beijing Engineering Research Center of Textile Nano Fiber, Beijing Institute of Fashion Technology, Beijing 100029, China; [orcid.org/0000-0001-5886-3261](https://orcid.org/0000-0001-5886-3261); Email: [clywangrui@bift.edu.cn](mailto:clywangrui@bift.edu.cn)

### Authors

**Yuhang Wu** – School of Materials Design and Engineering, Beijing Institute of Fashion Technology, Beijing 100029, China

**Guocong Ma** – School of Materials Design and Engineering, Beijing Institute of Fashion Technology, Beijing 100029, China

**Anying Zhang** – School of Materials Design and Engineering, Beijing Institute of Fashion Technology, Beijing 100029, China; School of Material Science and Engineering, Tiangong University, Tianjin 300387, China; [orcid.org/0000-0001-5189-759X](https://orcid.org/0000-0001-5189-759X)

**Weiwu Gu** – School of Materials Design and Engineering, Beijing Institute of Fashion Technology, Beijing 100029, China

Complete contact information is available at: <https://pubs.acs.org/doi/10.1021/acsomega.2c05324>

## Author Contributions

Y.W. and G.M. contributed equally to this work. Y.W., G.M., A.Z., W.G., R.W., and J.W. conceived the study and designed the experiments. A.Z. synthesized PET-CDs. Y.W., G.M., W.G., R.W., and J.W. wrote the manuscript with the assistance of all other co-authors.

## Notes

The authors declare no competing financial interest.

## ■ ACKNOWLEDGMENTS

This work was financially supported by the Beijing Municipal Natural Science Foundation (2222054), the Science and Technology Plan of Beijing Municipal Education Commission (KM202110012007), the Special Fund for High-level Teacher Team Construction of Beijing Institute of Fashion Technology (BIFTXJ202225), the Beijing Scholars Program (RCQJ20303), the Beijing Institute of Fashion Technology 2022 Postgraduate Education Quality Improvement Special Project, and the General Teaching Reform Project (120301990132).

## ■ ABBREVIATIONS

CDs, carbon dots; PET-CDs, PET-based carbon dots

## ■ REFERENCES

- (1) Barnard, E.; Arias, J. J. R.; Thielemans, W. Chemolytic depolymerisation of PET: a review. *Green Chem.* **2021**, *23*, 3765–3789.
- (2) Ross, P. S.; Chastain, S.; Vassilenko, E.; Etemadifar, A.; Zimmermann, S.; Quesnel, S. A.; Eert, J.; Solomon, E.; Patankar, S.; Posacka, A. M.; Williams, B. Pervasive distribution of polyester fibres in the Arctic Ocean is driven by Atlantic inputs. *Nat. Commun.* **2021**, *12*, No. 106.
- (3) Tournier, V.; Topham, C. M.; Gilles, A.; David, B.; Folgoas, C.; Moya-Leclair, E.; Kamionka, E.; Desrousseaux, M. L.; Texier, H.; Gavalda, S.; Cot, M.; Guémard, E.; Dalibey, M.; Nomme, J.; Cioci, G.; Barbe, S.; Chateau, M.; André, I.; Duquesne, S.; Marty, A. An engineered PET depolymerase to break down and recycle plastic bottles. *Nature* **2020**, *580*, 216–219.
- (4) Wei, R.; Zimmermann, W. Microbial enzymes for the recycling of recalcitrant petroleum-based plastics: how far are we? *Microb. Biotechnol.* **2017**, *10*, 1308–1322.
- (5) Kawai, F.; Kawabata, T.; Oda, M. Current knowledge on enzymatic PET degradation and its possible application to waste stream management and other fields. *Appl. Microbiol. Biotechnol.* **2019**, *103*, 4253–4268.
- (6) Moyses, D. N.; Teixeira, D. A.; Waldow, V. A.; Freire, D. M. G.; Castro, A. M. Fungal and enzymatic bio-depolymerization of waste post-consumer poly(ethylene terephthalate) (PET) bottles using *Penicillium* species. *3 Biotech* **2021**, *11*, No. 435.
- (7) Castro, A. M.; Carniel, A.; Menezes, S. M.; Chinellato, L. S., Jr.; Honorato, H.; Lima, A. P.; Chaves, E. G. Biocatalytic depolymerization of waste polyester mooring lines from oil and gas offshore platforms made of poly(ethylene terephthalate) (PET). *J. Appl. Chem. Biotechnol.* **2021**, *97*, 709–718.
- (8) Sadler, J. C.; Wallace, S. Microbial synthesis of vanillin from waste poly(ethylene terephthalate). *Green Chem.* **2021**, *23*, 4665–4672.

- (9) Karanastasis, A. A.; Safin, V.; Pitet, L. M. Bio-Based Upcycling of Poly(ethylene terephthalate) Waste for the Preparation of High-Performance Thermoplastic Copolyesters. *Macromolecules* **2022**, *55*, 1042–1049.
- (10) Zhou, H.; Ren, Y.; Li, Z.; Xu, M.; Wang, Y.; Ge, R.; Kong, X.; Zheng, L.; Duan, H. Electrocatalytic upcycling of polyethylene terephthalate to commodity chemicals and H<sub>2</sub> fuel. *Nat. Commun.* **2021**, *12*, No. 4679.
- (11) Song, C.; Zhang, B.; Hao, L.; Min, J.; Liu, N.; Niu, R.; Gong, J.; Tang, T. Converting poly(ethylene terephthalate) waste into N-doped porous carbon as CO<sub>2</sub> adsorbent and solar steam generator. *Green Energy Environ.* **2022**, *7*, 411–422.
- (12) Miao, S.; Liang, K.; Zhu, J.; Yang, B.; Zhao, D.; Kong, B. Hetero-atom-doped carbon dots: Doping strategies, properties and applications. *Nano Today* **2020**, *33*, No. 100879.
- (13) Zhang, Z.; Yi, G.; Li, P.; Zhang, X.; Fan, H.; Zhang, Y.; Wang, X.; Zhang, C. A minireview on doped carbon dots for photocatalytic and electrocatalytic applications. *Nanoscale* **2020**, *12*, 13899–13906.
- (14) Naik, V. M.; Bhosale, S. V.; Kolekar, G. B. A brief review on the synthesis, characterisation and analytical applications of nitrogen doped carbon dots. *Anal. Methods* **2022**, *14*, 877–891.
- (15) Atabaev, T. S. Doped Carbon Dots for Sensing and Bioimaging Applications: A Minireview. *Nanomaterials* **2018**, *8*, No. 342.
- (16) Zhang, Y.; Wu, Y.; Wang, J.; Hu, Y.; Fang, W.; Dang, J.; Wu, Y.; Li, X.; Zhao, H.; Li, Z. Optimization of Ionic Liquid-Mediated Red-Emission Carbon Dots and Their Imaging Application in Living Cells. *ACS Sustainable Chem. Eng.* **2020**, *8*, 16979–16989.
- (17) Yang, Z.; Xu, M.; Liu, Y.; He, F.; Gao, F.; Su, Y.; Wei, H.; Zhang, Y. Nitrogen-doped, carbon-rich, highly photoluminescent carbon dots from ammonium citrate. *Nanoscale* **2014**, *6*, 1890–1895.
- (18) Niu, X.; Zheng, W.; Song, T.; Huang, Z.; Yang, C.; Zhang, L.; Li, W.; Xiong, H. Pyrolysis of single carbon sources in SBA-15: A recyclable solid phase synthesis to obtain uniform carbon dots with tunable luminescence *Chin. Chem. Lett.* **2022**, DOI: 10.1016/j.ccllet.2022.05.074.
- (19) Li, Z.; Yu, H.; Bian, T.; Zhao, Y.; Zhou, C.; Shang, L.; Liu, Y.; Wu, L.-Z.; Tung, C.-H.; Zhang, T. Highly luminescent nitrogen-doped carbon quantum dots as effective fluorescent probes for mercuric and iodide ions. *J. Mater. Chem. C* **2015**, *3*, 1922–1928.
- (20) Sun, X.; Brückner, C.; Lei, Y. One-pot and ultrafast synthesis of nitrogen and phosphorus co-doped carbon dots possessing bright dual wavelength fluorescence emission. *Nanoscale* **2015**, *7*, 17278–17282.
- (21) Architha, N.; Ragupathi, M.; Shobana, C.; Selvakumar, T.; Kumar, P.; Lee, Y. S.; Selvan, R. K. Microwave-assisted green synthesis of fluorescent carbon quantum dots from Mexican Mint extract for Fe(3+) detection and bio-imaging applications. *Environ. Res.* **2021**, *199*, No. 111263.
- (22) Bi, X.; Hou, X.; Zhang, X.; Liu, W.; Ren, G.; Xu, S.; Wang, H.; Wei, W. Facile Synthesis of Green Fluorescent Carbon Dots and Application for Iron(III) Detection, Patterning and Cell Imaging. *ChemistrySelect* **2021**, *6*, 3729–3736.
- (23) Zhang, X.-Y.; Li, Y.; Wang, Y.-Y.; Liu, X.-Y.; Jiang, F.-L.; Liu, Y.; Jiang, P. Nitrogen and sulfur co-doped carbon dots with bright fluorescence for intracellular detection of iron ion and thiol. *J. Colloid Interface Sci.* **2022**, *611*, 255–264.
- (24) Song, Y.; Qi, N.; Li, K.; Cheng, D.; Wang, D.; Li, Y. Green fluorescent nanomaterials for rapid detection of chromium and iron ions: wool keratin-based carbon quantum dots. *RSC Adv.* **2022**, *12*, 8108–8118.
- (25) Kalanidhi, K.; Nagaraaj, P. Facile and Green synthesis of fluorescent N-doped carbon dots from betel leaves for sensitive detection of Picric acid and Iron ion. *J. Photochem. Photobiol., A* **2021**, *418*, No. 113369.
- (26) Wei, J.; Hao, D.; Wei, L.; Zhang, A.; Sun, C.; Wang, R. One-step preparation of red-emitting carbon dots for visual and quantitative detection of copper ions. *Luminescence* **2021**, *36*, 472–480.
- (27) Wang, R.; Gu, W.; Liu, Z.; Liu, Y.; Ma, G.; Wei, J. Simple and Green Synthesis of Carbonized Polymer dots from Nylon 66 Waste Fibers and its Potential Application. *ACS Omega* **2021**, *6*, 32888–32895.
- (28) Wei, J.; Yuan, Y.; Li, H.; Hao, D.; Sun, C.; Zheng, G.; Wang, R. A novel fluorescent sensor for water in organic solvents based on dynamic quenching of carbon quantum dots. *New J. Chem.* **2018**, *42*, 18787–18793.
- (29) Wei, J.; Li, H.; Yuan, Y.; Sun, C.; Hao, D.; Zheng, G.; Wang, R. A sensitive fluorescent sensor for the detection of trace water in organic solvents based on carbon quantum dots with yellow fluorescence. *RSC Adv.* **2018**, *8*, 37028–37034.
- (30) Rao, L.; Zhang, Q.; Wen, M.; Mao, Z.; Wei, H.; Chang, H.-J.; Niu, X. Solvent regulation synthesis of single-component white emission carbon quantum dots for white light-emitting diodes. *Nanotechnol. Rev.* **2021**, *10*, 465–477.
- (31) Chang, Q.; Zhou, X.; Xiang, G.; Jiang, S.; Li, L.; Wang, Y.; Li, Y.; Cao, Z.; Tang, X.; Ling, F.; Luo, X. Full color fluorescent carbon quantum dots synthesized from triammonium citrate for cell imaging and white LEDs. *Dyes Pigm.* **2021**, *193*, No. 109478.
- (32) Lu, Y.; Gao, H.; Chen, B.; Xue, Z.; Shang, Y.; Xu, J.; Yin, W.; Yang, T.; Li, X.; Chen, G. Synthesis and photoluminescence properties of orange-red carbon dots from the paper tissues as the precursor. *Appl. Opt.* **2022**, *61*, 2118–2124.